ELSEVIER

Journal of Organometallic Chemistry 637–639 (2001) 182–190

Journal of Organometallic Chemistry

www.elsevier.com/locate/jorganchem

(Ferrocenylmethyl)trialkyl ammoniums as template cations in optically active two-dimensional oxalate bridged [Cr–Mn] and [Cr–Ni] molecule-based magnets: synthesis and magnetic properties

Bernard Malézieux [a,*], Román Andrés [a], Muriel Brissard [a], Michel Gruselle [a], Cyrille Train [a], Patrick Herson [a], Ludmila L. Troitskaya [b], Viatcheslav I. Sokolov [b], Svetlana T. Ovseenko [b], Tatiana V. Demeschik [b], Nikolay S. Ovanesyan [c], Irina A. Mamed'yarova [d]

[a] *Laboratoire de Chimie Inorganique et Matériaux Moléculaires, Unité CNRS 7071, Université Pierre et Marie Curie, 4 Place Jussieu, Case 42, 75252 Paris Cédex 05, France*

[b] *INEOS, Nesmeyanov Institute of Organo-Element Compounds, Russian Academy of Sciences, Vavilov Street, 28, 117813 Moscow, Russia*

[c] *Institute of Problem of Chemical Physics, Russian Academy of Sciences, 142432 Chernogolovka, Russia*

[d] *Laboratory of Radiation and Photo Processes, Azerbaijan Academy of Sciences, Huseyn Djavid 31A, 370073 Bakou, Azerbaijan*

Received 20 December 2000; received in revised form 11 February 2001; accepted 7 March 2001

Abstract

A series of (ferrocenylmethyl)trialkyl ammoniums: $FcCH_2NR_3^+$ with $R = CH_3$ (**1**), C_2H_5 (**2**), n-C_3H_7 (**3**), n-C_4H_9 (**4**) (X-ray structure provided), n-C_5H_{11} (**5**) and the planar chiral 1,2-disubstituted $Fc(CH_3)CH_2NBu_3^+$ (**6**) have been tentatively used as template cation in order to synthesise bidimensional (2D) oxalate bridged molecule-based magnets of general formula $\{[Cr^{III}M^{II}(ox)_3][FcCH_2NR_3]\}_n$ and $\{[Cr^{III}M^{II}(ox)_3][Fc(CH_3)CH_2NBu_3]\}_n$ ($M = Mn^{2+}$, Ni^{2+}, $ox = C_2O_4^{2-}$). These polymeric compounds were obtained only for reactions performed with **2**, **3**, **4** and **6**. Starting from resolved $Cr(ox)_3^{3-}$, the networks were prepared in their two enantiomeric forms in the case of $\{[Cr^{III}Ni^{II}(ox)_3][FcCH_2NBu_3]\}_n$ ($[Cr_\Delta–Ni_\Lambda]$-**4** and $[Cr_\Lambda–Ni_\Delta]$-**4**) or $\{[Cr^{III}Mn^{II}(ox)_3][FcCH_2NBu_3]\}_n$ ($[Cr_\Delta–Mn_\Lambda]$-**4** and $[Cr_\Lambda–Mn_\Delta]$-**4**)) and characterised by circular dichroism measurements. All these compounds are ferromagnets with a Curie temperature close to 6 K when M = Mn and to 17 K for Ni. While the manganese [Cr–Mn] containing compounds are soft magnets, the [Cr–Ni] networks show coercive force up to 2200 Oe far above those previously reported for these networks.

Keywords: Ferrocenyl; Chirality; Circular dichroism; Chromium; Oxalate bridge; Molecule-based magnet

1. Introduction

The oxalate complexes chemistry has been particularly developed in the search of new molecule-based magnets. In this way, numerous polymeric bimetallic phases were reported in the literature [1]. Most of these studies focused on two-dimensional oxalate-based networks of general formula $\{[M_1^{III}M_2^{II}(ox)_3]A\}_n$ (A^+ = phosphonium, arsenium or ammonium). These bimetallic polymers were structurally and magnetically described [2]. The structural features of these compounds were abundantly discussed in the literature and various X-ray diffraction studies were published. They have provided evidence of the 2D character of these polymers. In general, the space group was found to be $R3c$ [3]. Nevertheless, it was reported that the compound $\{[Fe^{III}Mn^{II}(ox)_3][N(nC_5H_{11})_4]\}_n$ crystallises in the orthorhombic $C222_1$ space group [4]. Besides these examples, another trend appeared recently in the design of the 2D networks. The anionic magnetic network is used as a host-framework for cationic counterparts

* Corresponding author. Fax: +33-1-44273841.
E-mail address: malezieu@ccr.jussieu.fr (B. Malézieux).

0022-328X/01/$ - see front matter
PII: S0022-328X(01)00902-0

with particular optical or electronic properties in order to obtain new hybrid lamellar materials possessing both magnetic, electronic or non-linear optical properties. To this end were used: bedt-ttf [5], metallocenium [6,7] and 2,4-methoxy-*N*-heptylstilbazolium [8] ions.

The bidimensionality of the oxalate bridged layers results from the alternated configurations between two adjacent metallic centres according to the well-known propeller-like chirality of such hexa-coordinated compounds (Fig. 1).

In all the previous examples incorporating chromium, racemic $[Cr^{III}(ox)_3]^{3-}$ was used as anionic building block and combined in the polymer to an achiral cation. Since the compounds were synthesised from racemic mixtures it can be assumed, that the final materials remain racemic. Nevertheless, we have shown recently that such 2D networks can be obtained in optically active forms using resolved Δ or Λ tris(oxalato)chromate [9].

The assembling of the 2D networks consists in a succession of negatively charged honeycomb structure sheets separated by the cationic counter-parts. The cations usually selected to template 2D networks are often symmetric tetra-alkyl ammonium derivatives. The size of this cation plays a first order role in the formation of bimetallic oxalate co-ordinated networks: in the tetraalkyl series $N(C_nH_{2n+1})^{4+}$ it was mentioned that a polymeric compound was exclusively obtained for $n=$ 3, 4, 5 but never for 1, 2, 6, 7. On another hand, in the case of benzyltrialkyl ammonium derivatives, which present a more disymmetric geometry, the reaction was only described for $n=3$ [10]. The structural consequence of the choice of this counter-ion was discussed in terms of influence on the inter-layer distances and, on the solid-state organisation of the network itself. According to magnetic measurements, no significant or only little shifts were observed on the Curie temperature (T_c), leading to the conclusion that the anionic layers can be considered as independent units [3c,d]. Dealing with our investigation program on the search of new optically active magnetic materials, it was of interest to study the capability of tris(oxalato)-chromate-based networks to accommodate cationic molecules belonging to the ferrocene family. These molecules present several interesting features: stability, wide variety of compounds and can display planar chirality when they are 1,2 or 1,3 hetero-disubstituted.

This work focuses on the ability of various (ferrocenylmethyl)trialkyl ammonium cations to template the formation of anionic 2D bimetallic oxalate. The butyl derivative, for which X-ray structure analysis was obtained, has been used for the enantiomeric synthesis of optically active networks. The magnetic properties of this all set of compounds were systematically investigated.

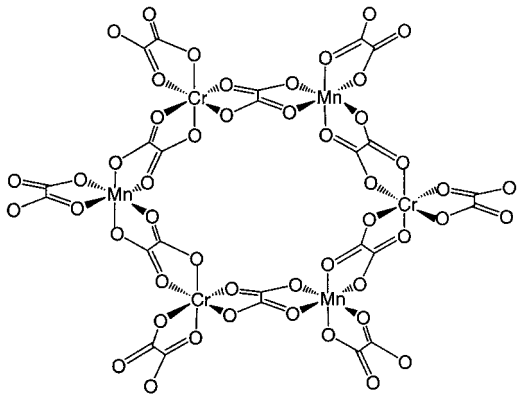

Fig. 1. Schematic drawing of graphite-like structure of 2D [CrMn(ox)$_3$] bridged network, only the plane with [Cr_Λ–Mn_Δ] is shown.

Table 1
Selected bond lengths (Å) and bond angles (°) of cation (**4**) iodide

Bond lengths			
N(1)–C(11)	1.53(1)	N(1)–C(12)	1.52(1)
N(1)–C(16)	1.51(1)	N(1)–C(20)	1.52(1)
C(12)–C(13)	1.51(1)	C(13)–C(14)	1.54(1)
C(14)–C(15)	1.50(2)	C(16)–C(17)	1.53(1)
C(17)–C(18)	1.51(1)	C(18)–C(19)	1.49(2)
C(20)–C(21)	1.52(1)	C(21)–C(22)	1.46(2)
C(22)–C(23)	1.49(2)		
Bond angles			
C(11)–N(1)–C(12)	109.5(6)	C(11)–N(1)–C(16)	110.9(6)
C(12)–N(1)–C(16)	105.9(6)	C(11)–N(1)–C(20)	106.0(6)
C(12)–N(1)–C(20)	112.0(6)	C(16)–N(1)–C(20)	112.7(7)
N(1)–C(11)–C(1)	114.2(7)	N(1)–C(12)–C(13)	114.4(7)
C(12)–C(13)–C(14)	109.7(8)	C(13)–C(14)–C(15)	110.9(10)
N(1)–C(16)–C(17)	114.8(7)	C(16)–C(17)–C(18)	109.2(8)
C(17)–C(18)–C(19)	113.3(11)	N(1)–C(20)–C(21)	115.1(7)
C(20)–C(21)–C(22)	111.6(8)	C(21)–C(22)–C(23)	113.0(11)

2. Results and discussion

2.1. Crystal structure of (ferrocenylmethyl)tributyl ammonium iodide (4)

Suitable single crystals for X-ray studies were obtained by slow evaporation of an acetone–ether solution (1:3) of the iodide salt of **4**. Selected bond lengths and angles are shown in Table 1. A CAMERON view of **4** is presented in Fig. 2.

The four chains bonded to the N atoms are disposed as far as possible from each other. The arm bearing the amino group with its three aliphatic chains is above the Cp-substituted plane, in opposition to the iron atom.

Considering the angle between the average planes containing the C(22)C(21)C(20)N and the C(21)C(20)NC(11) bonds sequences, a very weak value of 7.17° allowed to deduce the quasi-linear geometry of the CH_2 of the aliphatic chain extended towards the

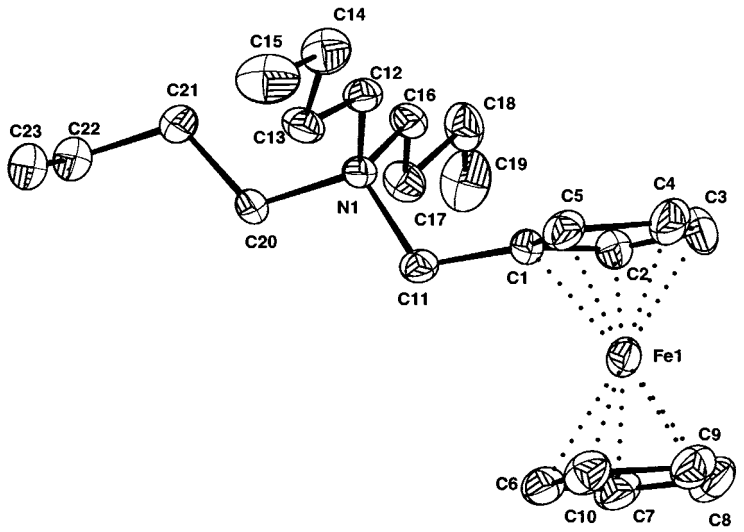

Fig. 2. Molecular structure of (ferrocenylmethyl)tributyl ammonium (**4**) iodide showing the atom-numbering system.

C(1)C(11) axis. Furthermore, this plane appears as almost perpendicular (92.6°) to that of the Cp substituted ring. The measure of the difference between the average planes occupied by the two *n*-butyl chains disposed from both sides of the plane perpendicular to that of the Cp ring revealed a very low angle of 6.28°. Thus a schematic drawing of a top view of the molecule would consist in a quasi-perfect cross whose centre would be the *N* atom and one extremity occupied by the ferrocenyl moiety. The only divergence from full-cross symmetry is due to the bend character of a terminal alkyl chain since a dihedral angle of 22.35° was found concerning the C(23)C(22)C(21)C(20) sequence.

2.2. Racemic polymers

Polymeric compounds: $\{[Cr^{III}M^{II}(ox)_3][FcCH_2NR_3]\}_n$ ([Cr–Mn], [Cr–Ni]-**2**, -**3** or -**4**) and $\{[Cr^{III}M^{II}(ox)_3]$-$[Fc(CH_3)CH_2NBu_3]\}_n$. ([Cr–Mn], [Cr–Ni]-**6**) were obtained starting from an equimolar mixture of $[Cr(ox)_3]^{3-}$ with a M^{II} salt (Mn^{2+} or Ni^{2+}) and an excess of the corresponding (ferocenylmethyl)-triethyl (**2**), -tri(npropyl) (**3**), -tri(*n*-butyl) (**4**) ammonium or the planar chiral 1,2-disubstituted $Fc(CH_3)CH_2NBu_3^+$ (**6**). Other experiments performed with -trimethyl (**1**) or -tri(*n*-pentyl) (**5**) ammonium salts failed. These results are very close to those previously reported for NR_4 salts that only reacted for R = *n*-propyl, *n*-butyl or *n*-pentyl and never when R = methyl, ethyl, hexyl or heptyl [10]. As a general trend, ammonium salts with short aliphatic chains of one or two carbons did not lead to the formation of polymeric compounds. This difference can be attribute to the relative bulky size of the $FcCH_2$– moiety, compared to a linear C_4 alkyl chain.

Previous studies on polymeric assemblies with ammonium salts showed the trend of the tetrahedral four arms cationic entities to adopt a tripodal disposition for three arms while the fourth extends into a cavity of the oxalate layer [11]. The asymmetric benzyltributyl ammonium cation integrates the oxalate network through the partial fitting of the benzylic fragment perpendicular to the anionic layer [10]. Conversely, it has been reported in consanguineous networks obtained with the decamethylferrocenium ion, that this latter was not located in the anionic hexagons formed by the oxalate sequence but remains in the inter-anionic layer as counter cation [12]. Interestingly, and in sharp contrast with the *N*-tetrabutyl analogues, the ferrocenic polymers appear to be water-soluble. The water solubility of two-dimensional oxalate networks has also been observed in the case of stibazolium derivatives. In these examples, X-ray crystal diffraction studies has revealed in some cases the behaviour of the guest cationic molecule as being independent units, while in other cases a partial insertion of an ethyl group in the oxalate layer was found [13]. Preliminary, X-ray powder diffraction analyses performed on the series [Cr–Mn]-**2**, -**3** and -**4** showed an increasing inter-layer anionic distance from 9.0 to 10.0 Å. These values match very well with previous related reports (8.95 Å for $\{[CrMn(ox)_3]$-$NBu_4\}_n$ [3a] and 9.43 Å for $\{[FeMn(ox)_3]PhCH_2NBu_3\}_n$ [10]). Size considerations are also valid for the planar chiral 1,2-disubstituted ferrocenic ammonium salt **6**. The presence of a methyl group on the cyclopentadienyl ring does not affect the properties of this molecule which behaviour (including the magnetic one of the resulting 2D network) remains similar to that of unsubstituted compound **4**. It is worth to mention that this new type of chiral cationic entity opens the way to a novel generation of 2D bimetallic networks able to

present optically active characters resulting from both the anionic and the cationic sub-lattices.

In conclusion, the size of the ferrocenic part allows it to play the role of a spacer between the negative charged planes and could explain the ability of the entitled series of compounds to act as template in polymeric networks even in the case of the triethyl derivative since simple tetraethyl ammonium could not.

2.3. Optically active polymers

The synthetic strategy developed to control the overall configurations requires the use of resolved chiral building blocks. In the reaction described above, starting from the following reagents: $FcCH_2NR_3^+$, M^{II}, $[Cr(ox)_3]^{3-}$ only the latter can introduced the chiral character of the network and also can be resolved in its two Δ and Λ enantiomers [14b].

We demonstrated previously [9], that when the polymers are prepared with resolved tris(oxalato)chromate(III) in conditions of rapid precipitation to prevent any racemisation process [14], it is possible to obtain optically active 2D networks. In a similar procedure, mixing solutions of optically active Δ or Λ $[Cr(ox)_3]^{3-}$ with Mn^{2+} or Ni^{2+} and the ferrocenic ammonium salt **4** results in the fast precipitation of the expected optically active polymers.

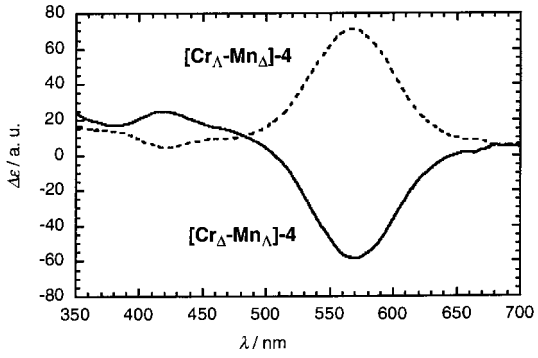

Fig. 3. Circular dichroism spectra of $[Cr_\Delta–Mn_\Lambda]$-**4** and $[Cr_\Lambda–Mn_\Delta]$-**4** in KBr dispersions.

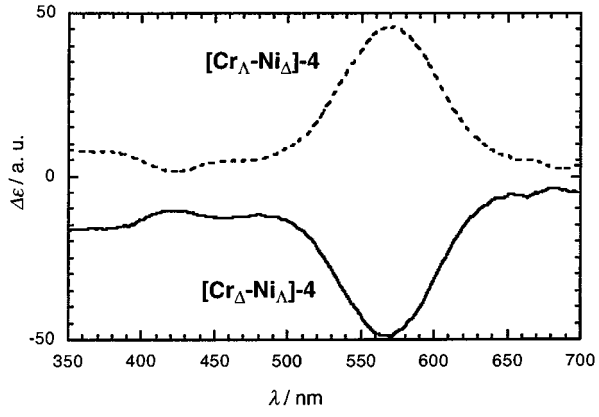

Fig. 4. Circular dichroism spectra of $[Cr_\Delta–Ni_\Lambda]$-**4** and $[Cr_\Lambda–Ni_\Delta]$-**4** in KBr dispersions.

Circular dichroism (CD) measurements were performed to assess the enantiomeric character of the obtained polymers and to ascribe the absolute configurations of the propeller-like metallic centres.

The couples of polymers $[Cr_\Lambda–Mn_\Delta]$-**4**, $[Cr_\Delta–Mn_\Lambda]$-**4** and $[Cr_\Lambda–Ni_\Delta]$-**4**, $[Cr_\Delta–Ni_\Lambda]$-**4** showed optical activity, displaying CD curves of the two opposite types. The CD spectra (Figs. 3 and 4) exhibit Cotton effects for the bands in the visible region, easily assigned to Cr^{III} d–d transitions. Further, characteristic very weak spin-forbidden bands were also observed [15].

Polymer $[Cr_\Lambda–Mn_\Delta]$-**4** obtained from $[Cr_\Lambda(ox)_3]^{3-}$ ($\lambda_{max} = 550$ nm) shows the same positive Cotton effect at $\lambda_{max} = 565$ nm. Polymer $[Cr_\Delta–Mn_\Lambda]$-**4** obtained from $[Cr_\Delta(ox)_3]^{3-}$ displays the corresponding negative Cotton effect at the same wavelength. The 15 nm difference observed between $[Cr_\Lambda(ox)_3]^{3-}$ and $[Cr_\Lambda–Mn_\Delta]$-**4** results from the shift in electronic absorption frequency is due to the bridging character of the co-ordinative oxalate ligand in the 2D network. The bands due to the Mn^{II} ion are too weak to be observed and probably hidden by the more intense bands due to the chromium. If the same 2D arrangement is maintained by these enantiomers, as it is expected to be, in accordance with the structural data, then the configurations of Mn centres should be the opposite to that of Cr centres.

The curves obtained for polymer $[Cr_\Lambda–Ni_\Delta]$-**4** prepared from $[Cr_\Lambda(ox)_3]^{3-}$ ($\lambda_{max} = 550$ nm) show the same positive Cotton effect at $\lambda_{max} = 565$ nm. Polymer $[Cr_\Delta–Ni_\Lambda]$-**4** obtained from $[Cr_\Delta(ox)_3]^{3-}$ displays the corresponding negative Cotton effect at the same wavelength. We feel that one should be cautious in attributing the weak bands belonging to the nickel and eclipsed by that of the chromium.

2.4. Magnetic measurements

To determine the nature of the exchange interaction between the two oxalate transition metal ions, we plot χT versus T in the paramagnetic region (Fig. 5). These curves show a monotonic variation corresponding to a ferromagnetic interaction for all the [Cr–Mn] and [Cr–Ni] compounds. This result is confirmed by the χ^{-1} versus T curves (insert of Fig. 5). These curves are linear for temperature ranging between 30 and 300 K and can be fitted using a Curie–Weiss law $\chi^{-1} = (T - \Theta)/C$. The Curie constants deduced from susceptibility measurements are listed in Table 2 as well as the Weiss constants Θ deduced from the fits. The latter give a quantitative measurement of the exchange interaction in these compounds.

When the temperature is lowered, all the studied compounds show a transition from a paramagnetic to a

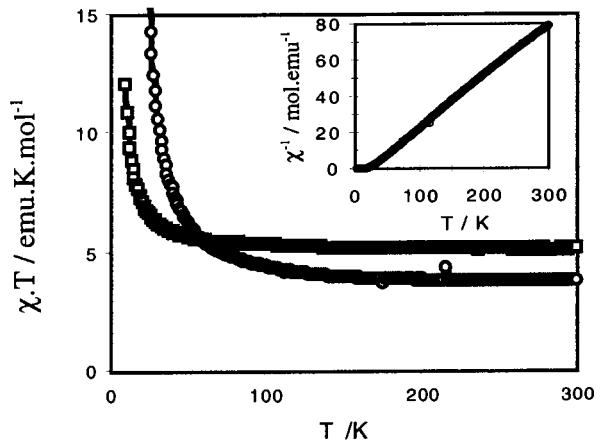

Fig. 5. χT vs. T curves for [CrMn]-**2** (open squares) and [CrNi]-**2** (open circles). The inset shows χ^{-1} vs. T for [CrNi]-**3** (H = 0.1 T in both graphs).

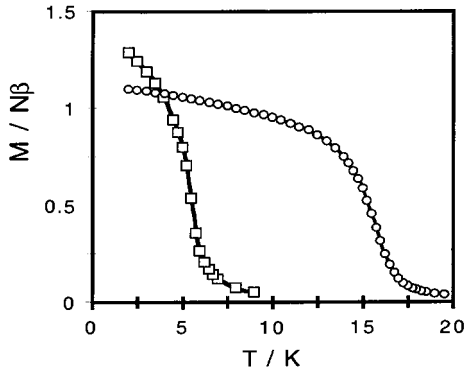

Fig. 6. Field-cooled ($H = 0.01$ T) curves for [CrMn]-**3** (open squares) and [CrNi]-**3** (open circles).

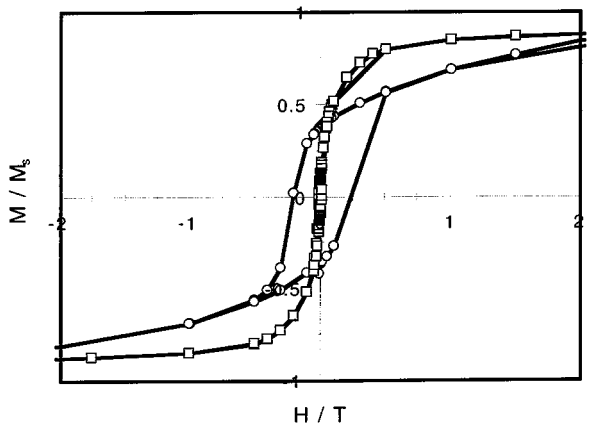

Fig. 7. Reduced magnetisation of [CrMn]-**3** (open squares) and [CrNi]-**3** (open circles) vs. field at 2 K.

long range ordered state (Fig. 6). To estimate the critical temperature T_c corresponding to this transition, we use the procedure consisting in considering the Curie temperature as the intersection of the linear fit of the steepest part of the field-cooled curve obtained in 0.01 T with the T axis (Table 2).

The hysteresis loops of the compounds have been measured at 2 K, far below the critical temperature (Fig. 7). [Cr–Mn] behave as very soft magnets while the coercive force of the [Cr–Ni] networks are above 2000 Oe (Table 2). The saturation magnetisations M_s are listed in Table 2.

Both the ferromagnetic nature of the exchange interaction through the oxalate bridge and the values of T_c and Θ are in accordance with those reported in the literature for oxalate bridged 2D networks [2]. A regular increase of T_c and Θ with the length of the alkyl chains of the ammonium cation seems to exist for the [Cr–Ni] series but such an evolution does not appear for the [Cr–Mn] series. As already stated [3c–10], it seems impossible to correlate the subtle changes in exchange interaction with the modifications of the structural parameters induced by an increasing size of the countercation.

The Curie constants of the [Cr–Ni] compounds are slightly higher than the one corresponding to one manganese and one chromium isolated ions. On the contrary, the saturation magnetisation is below the theoretical 5 μ_B per Cr–Ni unit. This behaviour could be tentatively explained by the presence of paramagnetic salts (like MCl_2) and/or oxalate bridged chains [1c] in the powders leading to an excess of spin carriers that are not ordered at low temperature. The initial paramagnetic salts are poorly eliminated from the final

Table 2
Summary of the magnetic data for the eight compounds: T_c, critical temperature, Θ, Weiss constant; C, Curie constant; M_c saturation magnetisation; and H_c, coercive field at 2 K

	T_c (K)	Θ (K)	C (emu K mol^{-1})	M_s (μ_B)	H_c (T)
[Cr–Mn]-**2**	5.5	5.5	5.1	6.25	–
[Cr–Mn]-**3**	6.2	7.6	6.3	7.20	–
[Cr–Mn]-**4**	5.3	5.6	6.0	7.20	–
[Cr–Mn]-**6**	5.3	5.3	7.0	8.20	–
[Cr–Ni]-**2**	16.3	20.8	3.1	4.45	0.21
[Cr–Ni]-**3**	16.6	20.9	3.1	4.34	0.21
[Cr–Ni]-**4**	17.1	19.5	3.3	3.60	0.20
[Cr–Ni]-**6**	17.0	25.6	3.7	4.64	0.22

product since the latter is water-soluble thus precluding successive water extraction.

The most striking feature in the magnetic properties of the studied compounds is the high coercive forces observed in the [Cr–Ni] series. The evolution of the coercive force when going from manganese to nickel can be attributed to the higher single-ion anisotropy of the latter. Nevertheless the coercive force of the [Cr–Ni] networks synthesised from the (ferrocenylmethyl)trialkyl ammonium is ten times as high as the value reported for the {[$NiCr(ox)_3$][NBu_4]} compound [2b].

High coercive forces are rarely reported for molecule-based magnets [7,12,16]. Shape anisotropy can play an important role. It has been identified as the main mechanism of the hardness of dicyanamide-based magnets [16]. Nevertheless the counter cation does not seem to play an innocent role: the use of cobalticinium as countercation led to an enhancement of the coercive force by a factor of two compared to NBu_4^+ or fericinium in {[$FeCr(ox)_3$]A} compounds [7]. The evolution observed here is even more impressive but the reasons of the increase are yet unclear.

In conclusion, the role of the counter-ion on the magnetic properties is not easy to establish. It can actually modify at least three essential crystallographic parameters — the inter-layer distance, the stacking of the layers and the distance and angles between the metallic centres within the layers. The latter parameter will be of particular importance since J and therefore Θ and T_c are mainly determined by the basic 'motif' encountered in these compounds, namely a metal ion in a pseudo-octahedral environment linked to the other one through three oxalate bridges [1b]. Further investigations including precise magnetostructural correlations and evaluation of particle size, shape and crystallimity will thus be needed to enlighten the mechanisms that drive the subtle modifications of the magnetic properties (T_c, H_c) when changing the cationic counterpart.

3. Experimental

3.1. General

The IR spectra were recorded on a Bio-Rad IRFT spectrometer as KBr pellets in the 4000–250 cm^{-1} region. Elemental analyses were completed at the SIARE-UPMC Paris. X-ray powder diffraction profiles were recorded at room temperature on an automated Philips diffractometer in reflexion mode with Fe–$K_{\alpha 1\alpha 2}$ radiations over the 10–60° (2Θ) angular range. Specific rotations of the starting materials were measured at 20 °C in a 1 dm tube containing the aqueous solutions, using the sodium D line in a polarimeter Ameria AA5. The enantiomeric excesses were calculated by comparison to the maximum specific rotation found in the literature [17]. CD spectra were recorded with a Jasco model J-710 spectropolarimeter. Measurements were performed on 13 mm standard diameter disks as dispersions of 0.1–1 mg of the resulting complexes over dried 100 mg KBr. The baseline correction was performed with the spectrum of pure KBr disk. Spectra were recorded for the wavelength range 700–200 nm. X-ray diffraction data. CD measurements were used to demonstrate the enantiomeric character of the two species and to determine the absolute configurations of the metallic centres. Absolute configurations for Cr centres were determined by comparison of their CD spectra with those of D and L enantiomers of potassium tris(oxalate)chromate(III) following the principle that two related optically active molecules have the same absolute configuration if they give a Cotton effect of the same sign in the absorption wavelength region of an electronic transition common to both molecules [15a, 18]. Due to the extremely low solubility of the obtained polymers, solid-state CD was imposed. This technique has been used to allow CD measurements in the case of compounds which racemise rapidly in solution. This method is useful mainly for qualitative comparisons because of the intensities in general vary with the individual samples [15b].

The magnetic moment of powdered samples were measured between 2 and 300 K either on a home-made (Orsay) or on a Quantum Design MPMS5 (Paris) SQUID magnetometer. The magnetic susceptibility was measured between 10 and 300 K. The zero field-cooled (ZFC), field-cooled (FC) and remnant magnetisation versus temperature are measured in a 0.01 T external field. The hysteresis loops were recorded at 2 K sweeping the field up to 5 T.

3.2. Synthesis

$K_3[Cr(ox)_3]\cdot 3H_2O$ was prepared according to literature methods [19]. Procedures of resolution already described have been followed to obtain Δ and Λ isomers of $[Cr(ox)_3]^{3-}$ [17]. The other reagents are commercially available and were used as purchased.

Preparations of the iodide or bromide salts of $FcCH_2NR_3^+$ with $R = CH_3$ (**1**); C_2H_5 (**2**); n-C_3H_7 (**3**); n-C_4H_9 (**4**); n-C_5H_{11} (**5**) as well as the 1,2-disubstituted salt $Fc(CH_3)CH_2NBu_3I$ (**6**) were prepared as described previously starting from ((*N*,*N*-dimethylamino)-methyl)ferrocene [20].

3.2.1. Preparation of [Cr–Mn]-2 and [Cr–Ni]-2

A methanolic solution (0.2 ml) of the iodide ammonium salt of **2** (0.0516 g, 0.12 mmol) was added to an aqueous solution (0.2 ml) of $(NH_4)_3Cr(ox)_3\cdot 3H_2O$ (0.0325 g, 0.08 mmol) and $MnCl_2\cdot 4H_2O$ (0.0163 g, 0.08 mmol). The mixture was left to react for 1 h to give a

fine green precipitate. After filtration (0.4 μm) and several washings by a (1:1) water–MeOH mixture (2 × 2 ml), pure MeOH then Et_2O, 0.020 g of [Cr–Mn]-**2** as a green pale powder was recovered (38% yield). The same procedure was followed for the preparation of [Cr–Ni]-**2** using $NiCl_2$ instead of $MnCl_2$. [Cr–Mn]-**2** Anal. Found: C, 40.38; H, 3.86; N, 1.98. Calc. for $C_{23}H_{26}NO_{12}CrFeMn$: C, 41.16; H, 3.90; N, 2.09%. [Cr–Ni]-**2** Found: C, 43.38; H, 3.69; N, 2.13. Calc. for $C_{23}H_{26}CrFeNNiO_{12}$: C, 40.93; H, 3.88; N, 2.08%. IR (KBr, cm^{-1}): [Cr–Mn]-**2**: 1631, vs; 819, w; 804, w. [Cr–Ni]-**2**: 1623, vs; 822, w; 806, w.

3.2.2. Preparation of [Cr–Mn]-3 and [Cr–Ni]-3

Polymers [Cr–Mn]-**3** and [Cr–Ni]-**3** were prepared in a similar fashion to that described for polymer [Cr–Mn]-**2** and [Cr–Ni]-**2** (30% yield). [Cr–Mn]-**3** Anal. Found: C, 41.68; H, 4.47; N, 2.36. Calc. for $C_{26}H_{32}CrFeMnNO_{12}$: C, 43.78; H, 4.52; N, 1.96%. [Cr–Ni]-**3** Found: C, 43.38; H, 4.69; N, 2.13. Calc. for $C_{26}H_{32}CrFeNNiO_{12}$: C, 43.55; H, 4.50; N, 1.95%. IR (KBr, cm^{-1}): [Cr–Mn]-**3** 1626, vs; 819, w; 804, w. [Cr–Ni]-**3**: 1623, vs; 822, w; 806, w.

Table 3
Crystal data and structure refinement parameters for cation (**4**) iodide

Empirical formula	$C_{23}H_{38}NFeI$
Formula weight ($g\,mol^{-1}$)	511.32
Temperature (K)	295
Crystal system	Monoclinic
Space group	$P2_1/c$
Crystal shape	Parallelepiped
Crystal colour	Yellow
Unit cell dimensions	
a (Å)	10.424 (5)
b (Å)	15.057 (16)
c (Å)	15.586 (15)
β (°)	94.59 (6)
V (Å^3)	2438 (4)
Z	4
Absorption coefficient μ (cm^{-1})	18.77
Density ρ ($g\,cm^{-3}$)	1.39
Diffractometer	Enraf–Nonius Cad 4
Radiation	Mo–K_α ($\lambda = 0.71069$ Å)
Scan type	$2\theta/\omega$
Scan range (°)	$0.8 + 0.345\ \mathrm{tg}\theta$
Theta range for data collection (°)	1–25
Octants collected	0, 12; 0, 17; −18, 18
Reflections collected	4730
Number of unique data collected	4282
Number of data collected for refinement	2421
Merging R	0.039
Decay of standards reflexions (%)	7.6
$R = \Sigma\|\|F_o\| - \|F_c\|\|/\Sigma\|Of\|$	0.066
Rw [a] $= [\Sigma\, w(\|\|F_o\| - \|F_c\|\|)^2/\Sigma\, wF_o^2]^{1/2}$	0.080
Absorption correction	DIFABS ($T_{min} = 0.80$, $T_{max} = 1.28$)
Secondary extinction coefficient	434
Number of variables	237
$\Delta\rho_{min}$ (e Å^{-3})	−0.87
$\Delta\rho_{max}$ (e Å^{-3})	0.77
Goodness-of-fit on F^2	1.07

[a] $w = w'[1 - ((\|F_o\| - \|F_c\|)/6\sigma(F_o))^2]^2$ with $w' = 1/\Sigma_r T_r(X)$ with three coefficients for a Chebyshev series for which $X = F_c/F_c(\mathrm{max})$.

3.2.3. Preparation of [Cr–Mn]-4 and [Cr–Ni]-4

Polymers [Cr–Mn]-**4** and [Cr–Ni]-**4** were prepared in a similar fashion to that described for polymer [Cr–Mn]-**2** and [Cr–Ni]-**2**. [Cr–Mn]-**4** Anal. Found: C, 46.11; H, 4.71; N, 1.73. Calc. for $C_{29}H_{38}CrFeMnNO_{12}$: C, 43.34; H, 5.00; N, 1.93%. [Cr–Ni]-**4** Found: C, 43.14; H, 5.02; N, 1.78. Calcd for $C_{29}H_{38}CrFeNNiO_{12}$: C, 45.88; H, 5.00; N, 1.84%. IR (KBr, cm^{-1}): [Cr–Mn]-**4** 1628, vs; 819, w; 805, w. [Cr–Ni]-**4**: 1627, vs; 822, w; 805, w.

3.2.4. Preparation of the optically active [Cr_Λ–Mn_Λ]-4 and [Cr_Δ–Mn_Δ]-4

Note: the yields are not optimised taking into account the racemisation process of the optically active trisoxalate chromate in aqueous solution.

To a methanolic solution of the *bromide* ammonium salt of **4** (0.065 g in 0.2 ml, 0.12 mmol) was added an aqueous solution (0.2 ml) containing $MnCl_2{\cdot}4H_2O$ (0.030 g, 0.14 mmol). and the (Δ) or (Λ) $K_3Cr(ox)_3{\cdot}3H_2O$ (0.060 g, 0.12 mmol) ($[\alpha]_D = -1590$ or $[\alpha]_D = +1523$, respectively). The mixture is continuously scratched with a glass stick to provide a rapid precipitation of the polymer. The solution was filtered off (0.4 μm) and after two washings by a (1:1) water–MeOH mixture and then diethyl ether, 0.022 g of powder was recovered (33% yield).

3.2.5. Preparation of the optically active [Cr_Λ–Ni_Λ]-4 and [Cr_Δ–Ni_Λ]-4

The same procedure described for Mn analogues was adopted using $NiCl_2$ instead of $MnCl_2$

3.2.6. Preparation of [Cr–Mn]-6 and [Cr–Ni]-6

The same procedure described for [Cr–Mn]-**4** and [Cr–Ni]-**4** was used starting from **6**. (38 and 42% yield, respectively). [Cr–Mn]-**6** Anal. Found: C, 44.23; H, 4.15; N, 1.30. Calc. for $C_{30}H_{40}NO_{12}CrFeMn$: C, 46.83; H, 5.24; N, 1.82%. [Cr–Ni]-**6** Found: C, 45.01; H, 4.96; N, 1.56. Calcd for $C_{30}H_{40}CrFeNiNO_{12}$: C, 46.60; H, 5.21; N, 1.81%. IR (KBr, cm^{-1}): [Cr–Mn]-**6** 1629, vs; 805, w. [Cr–Ni]-**6**: 1624, vs; 822, w.

3.3. X-ray crystallography

Crystallographic data for **4** are given in Table 3. A selected single crystal was set up on an automatic diffractometer. Unit cell dimensions with estimated standard deviations were obtained from least-squares refinements of the setting angles of 25 well-centred reflections. Two standard reflections were monitored

periodically; they showed no change during data collection. Corrections were made for Lorentz and polarisation effects. Secondary extinction corrections were necessary. An empirical absorption based on DIFABS [21] was applied.

Computations were performed by using the PC version of CRYSTALS [22]. Atomic form factors for neutral N, C, Fe, H and I were taken from Ref. [23]. Real and imaginary parts of anomalous dispersion were taken into account. The structure was solved by direct methods (SHELXS86) [24] and successive Fourier maps. All non-hydrogen atoms were anisotropically refined.

Almost all hydrogen atoms have been seen on difference maps but they were introducing in calculated positions and only an overall isotropic thermal parameter was refined.

Least-square refinements in full-matrix were carried out by minimising the function $\Sigma w(F_o - |F_c|)^2$ where F_o and F_c are the observed and calculated structure factors. Models achieved convergence with $R = \Sigma(\|F_o - |F_c\|)/\Sigma w F_o$ and $Rw = [\Sigma w(F_o - |F_c|)^2/\Sigma w\ (F_o)^2]^{1/2}$ having values listed in Table 3.

In the last stages of the refinement, each reflection was assigned a weight: $w = w'[1 - (\|F_o| - |F_c\|)/6\sigma|F_o|)^2]^2$ with $w' = 1/-1A_rT_r(X)$ with coefficients 8.63, 0.132 and 6.69 for a Chebyshev series, for which $X = F_c/F_c(\max)$.

Criteria for a satisfactory complete analysis were the ratio of rms shift to standard deviations being less then 0.2 and no significant features in the difference map. The view of the molecule is done using CAMERON [25] (Fig. 2). Ellipsoids represent 20% of probability.

4. Supplementary material

Crystallographic data for the structural analysis have been deposited with the Cambridge Crystallographic Data Centre, CCDC no. 154349 for (ferrocenylmethyl)tributyl ammonium iodide. Copies of this information may be obtained free of charge from The Director, CCDC, 12 Union Road, Cambridge CB2 1EZ, UK (Fax: +44-1223-336033; e-mail: deposit@ccdc.cam.ac.uk or www: http://www.ccdc.cam.ac.uk).

Acknowledgements

We thank INTAS Project 96-903, l'université Pierre et Marie Curie, the CNRS for the financial support and the Spanish Ministerio de Educacion y cultura for a postdoctoral fellowship. The authors also thank I. Rosenman, P. Veillet, L. Reversat and J.P. Renard for easy access to their respective SQUID apparatus; M. Takahashi and T. Selmane for assistance in performing the CD measurements.

References

[1] (a) M. Julve, M. Verdaguer, A. Gleizes, M. Philoche-Levisalles, O. Kahn, Inorg. Chem. 23 (1984) 3808;
(b) O. Kahn, Angew. Chem. Int. Ed. Engl. 24 (1985) 834;
(c) O. Kahn, Molecular Magnetism, VCH, Weinheim, Germany, 1993;
(d) S. Decurtins, H.W. Schmalle, R. Pellaux, R. Huber, P. Fischer, B. Ouladdiaf, Adv. Mater. 8 (1996) 647;
(e) S. Decurtins, H.W. Schmalle, R. Pellaux, P. Fischer, A. Hauser, Mol. Cryst. Liq. Cryst. 305 (1997) 227.

[2] (a) Z.J. Zhong, N. Matsumoto, H. Okawa, S. Kida, Chem. Lett. (1990) 87;
(b) H. Tamaki, Z.J. Zhong, N. Matsumoto, S. Kida, M. Koikawa, N. Achiwa, Y. Hashimoto, H. Okawa, J. Am. Chem. Soc. 114 (1992) 6974;
(c) H. Okawa, N. Matsumoto, H. Tamaki, M. Ohba, Mol. Cryst. Liq. Cryst. 233 (1993) 257;
(d) J. Larionova, P. Monbelli, J Sanchez, O. Kahn, Inorg. Chem. 37 (1998) 679.

[3] (a) L.O. Atovmyan, G.V. Shilov, R.N. Lyuobovskaya, E.I. Zhilyaeva, N.S. Ovanesyan, S.I. Pirumova, I.G. Gusakovskaya, Y.G. Morozov, JETP Lett. 58 (1993) 766;
(b) S. Decurtins, H.W. Schmalle, H.R. Oswald, A. Linden, J. Ensling, P. Gütlich, A. Hauser, Inorg. Chim. Acta 216 (1994) 65;
(c) G.V. Shilov, L.O. Atovmyan, R.N.N.S. Ovanesyan, A.A. Pyalling, L. Bottyan, Russ. J. Coord. Chem. 24 (1998) 288;
(d) R. Pellaux, H.W. Schmalle, R. Huber, P. Fischer, T. Hauss, B. Ouladdiaf, S. Decurtins, Inorg. Chem. 36 (1997) 2301.

[4] S.G. Carling, C. Mathonière, P. Day, K.M. Abdul Malik, S.J. Coles, M.B. Hursthouse, J. Chem. Soc. Dalton Trans. (1996) 1839.

[5] (a) E. Coronado, J.R. Galan-Mascaros, C.J. Gomez-Garcia, Synth. Met. 102 (1999) 1459;
(b) E. Coronado, J.R. Galan-Mascaros, C.J. Gomez-Garcia, V.L. Laukhin, Nature 408 (2000) 407.

[6] H. Clemente-Leon, E. Coronado, J.R. Galan-Mascaros, C.J. Gomez-Garcia, Chem. Commun. (1997) 1727.

[7] (a) E. Coronado, J.R. Galan-Mascaros, C.J. Gomez-Garcia, R. Burriel, J. Magn. Magn. Mater. 196 (1999) 558;
(b) E. Coronado, J.R. Galan-Mascaros, C.J. Gomez-Garcia, J. Ensling, P. Gütlich, Chem. Eur. J. 6 (2000) 552.

[8] S. Bénard, Y. Pei, T. Coradin, E. Rivière, K. Nakatani, R. Clément, Adv. Mater. 9 (1997) 981.

[9] R. Andrés, M. Gruselle, B. Malézieux, M. Verdaguer, J. Vaissermann, Inorg. Chem. 38 (1999) 4637.

[10] C. Mathonière, C.J. Nuttall, S.G. Carling, P. Day, Inorg. Chem. 35 (1996) 1201.

[11] L.O. Atovmyan, G.V. Shilov, R.N. Lyuobovskaya, E.I. Zhilyaeva, N.S. Ovanesyan, O.A. Bogdanova, S.I. Perumova, Russ. J. Coord. Chem. 23 (1997) 640.

[12] E. Coronado, J.R. Galan-Mascaros, C.J. Gomez-Garcia, J.M. Martinez-Agudo, Adv. Mater. 11 (1999) 558.

[13] S. Bénard, PhD thesis. University of Orsay, 2000.

[14] (a) C.H. Johnson, Trans. Faraday Soc. 31 (1935) 1612;
(b) The tris(oxalate)chromato(III)ion $[Cr(ox)_3]^{3-}$ was the first resolved complex anion. See: A. Werner, Chem. Ber. 45 (1912) 061.

[15] (a) A.J. Mc Caffery, S.F. Mason, R.E. Ballard, J. Chem. Soc. (1965) 2883;
(b) R.D. Gillard, D.J. Shepherd, D.A. Tarr, J. Chem. Soc. Dalton Trans. (1976) 594.

[16] M. Kurmoo, C.J. Kepert, New J. Chem. (1998) 1515.

[17] (a) F.P. Dwyer, A.M. Sargeson, J. Phys. Chem. 60 (1956) 1331;
(b) G.B. Kauffman, L.T. Takahashi, N. Sugisaka, Inorg. Synth. 8 (1966) 207.

[18] (a) F.S. Richardson, Chem. Rev. 79 (1979) 17;
(b) M. Ziegler, A. von Zelewsky, Coord. Chem. Rev. 177 (1998) 257.
[19] J.C. Bailar, E.M. Jones, Inorg. Synth. 1 (1939) 37.
[20] L.L. Troitskaya, T.V. Demeshchik, V.I. Sokolov, I.A. Mamed'yarova, B. Malézieux, M. Gruselle, Russ. Chem. Bull. (2001), in preparation. To prepare the ammonium derivatives **1**–**5** an alternative is also possible using EtBr on DMAMF in acetone and refluxing the obtained bromide salt in acetonitrile with a three-fold excess of the corresponding trialkyl amine. It is noteworthy that this intermediary dimethyl ethylferrocenic ammonium bromide does not react to form 2D network.
[21] N. Walker, D. Stuart, Acta Crystallogr. Sect. A 39 (1983) 158 (DIFABS).
[22] D.J. Watkin, C.K. Prout, J.R. Carruthers, P.W. Betteridge, CRYSTALS Issue 10, Chemical Crystallography Laboratory, University of Oxford, UK, 1996.
[23] International Tables for X-ray Crystallography, vol. IV, Kynoch Press, Birmingham, 1974.
[24] G.M. Sheldrick, SHELXS86, Program for Crystal Structure Solution University of Göttingen, Germany, 1986.
[25] D.J. Watkin, C.K. Prout, L.J. Pearce, CAMERON, Chemical Crystallography Laboratory, University of Oxford, UK, 1996.